An Investigation of the Pump Operating Characteristics as a Novel Control Index for LVAD Control

Seongjin Choi, J. Robert Boston, and James F. Antaki

Abstract: This work presents a novel control index to regulate the pump speed of an axial flow blood pump for the left ventricular assist device (LVAD). The control index is based on the characterization of pump operating conditions such as normal or suction status. The pump operating characteristics reveal that a certain pulsatility relationship between the pump pressure difference and the pump flow is a unique index to identify the pump operating status under the diverse pump operating environments.

Keywords: Axial flow blood pump, control index, LVAD, pump characteristics.

1. INTRODUCTION

The left ventricular assist device (LVAD) is an implanted mechanical device, located in the left ventricle and the aorta, to support or replace a heart that has failed. The control of LVAD has been a difficult problem to formulate, since physiological variables in the body with an implanted pump are not clearly defined as control variables and the quantities of changes in control variables necessary to support a natural heart are not well defined, either [1]. In addition to the difficulty in problem formulation of LVAD control, the acquisition of the proper physiological information is very limited due to an inability of the implanted sensors, especially for long-term use [2].

The LVAD currently under investigation is an axial flow blood pump, a type of nonpulsatile blood pump. While it has the advantages of small size, efficiency, and reliability over pulsatile pumps, it requires improved pump speed control due to the characteristics of pump operation. It demonstrates poor sensitivity to the ventricular preload and good sensitivity to the ventricular afterload [3]. As the pump speed increases to provide more blood to the body while supporting the natural heart, the LVAD tries to drain the blood from the left ventricle regardless of the amount of blood available in the left ventricle. As a result, a high pump speed can induce suction in the left ventricle, which can cause damage to the myocardium, blood, and lungs. Suction avoidance is important to safely operate the blood pumps and it requires implanted sensors, unreliable for long-term use, to obtain the proper physiological information.

To deal with these difficult situations such as complex control problem formulation, non reliable sensors, and suction in the left ventricle, the controller for LVAD employs a sensorless approach to regulate the pump speed without introducing suction in the left ventricle [4]. The controller uses the pulsatility index of the pump flow estimate as a control index while the pump flow estimate is available through the developed pump model without implanted sensors [5]. Though the controller regulates the pump speed according to the reference pulsatility index of the pump flow, it has its own limitation of choice of the reference pulsatility index of the pump flow. As the pump speed increases to provide more blood to the body, the physiological variables such as the pump flow and other variables show diminishing pulsatilities before suction occurrence. However, the pulsatilities of the physiological variables increase after suction occurrence as the pump speed increases. The single value of the pulsatility index of the pump flow can indicate both “before suction” and “suction” of the pump operating status. That is, the reference pulsatility index of the pump flow as a reference control index for the controller should be well defined to support the natural heart. Otherwise, the pulsatility controller can introduce suction in the left ventricle with an excessively high pump speed. This problem leads to the suction detection approaches to provide a safe pump speed control while avoiding suction in the

Manuscript received October 5, 2004; revised February 11, 2005; accepted February 11, 2005. Recommended by Editorial Board member Sun Kook Yoo under the direction of Editor Keum-Shik Hong. This work was supported by Korea University Grant.

Seongjin Choi is with the Department of Electronics and Information Engineering, Korea University, Korea (e-mail: choisj@korea.ac.kr).

J. Robert Boston is with the Department of Electrical Engineering, University of Pittsburgh, U.S.A. (e-mail: boston@engr.pitt.edu).

James. F. Antaki is with the Department of Biomedical Engineering and Computer Science, Carnegie Mellon University, U.S.A. (e-mail: antaki@andrew.cmu.edu).

left ventricle [6-8].

In this paper, we investigate the pulsatility properties of the pump operating characteristics under different simulated physiological conditions. The pulsatility relationship between the pump flow and the pressure difference shows a unique property that can be used as a control index to adjust the pump speed safely without suction induction in the left ventricle.

2. MODEL OF A CARDIOVASCULAR SYSTEM WITH AN IMPLANTED LVAD

The model of a cardiovascular system with an implanted LVAD consists of the cardiovascular system model, suction model, and axial flow blood pump model as shown in Fig. 1 [9]. The model in Fig. 1 employs the electric circuit analogs of the lumped hydraulic model. The resistor, inductor, and capacitor represent the resistance of the blood flow, the inertance of the blood, and the compliance of the blood vessel wall, respectively. The diodes in the model represent the valves of the heart. The compliance of the ventricles is modeled as a time-varying capacitor. The time-varying compliance $C(t)$ in the left and right ventricles is given by

$$C(t) = \frac{1}{E(t)}, \tag{1}$$

where $E(t)$ is the elastance of the ventricles. The elastance function in (1) is modeled as

$$\begin{aligned} E(t) &= E_{\max}(1-\cos(2\pi t/t_s))/2 + E_{\min} && 0 \le t < t_s \\ &= E_{\min} && t_s \le t < t_c \end{aligned} \tag{2}$$

where t_s is a systolic period, t_c is a full cardiac period, and E_{max} and E_{min} are the maximum and the minimum values of elastance, respectively [10].

The suction model is based on the model in [11] and slightly modified. The suction model accounts for the suction phenomenon in the left ventricle during an excessive pump speed operation. The model of the axial flow blood pump under consideration was previously developed in [5] and is given by

$$\begin{aligned} J\frac{d\omega}{dt} &= \frac{3}{2}K_B I - B\omega - Q\omega(a_0\omega + a_1\omega^2), \\ H &= b_0 Q + b_1\frac{dQ}{dt} + b_2\omega^2, \end{aligned} \tag{3}$$

where J is the inertia of the rotor, K_B is the back EMF constant, B is the damping factor, respectively, I and ω are motor current and pump speed, respectively, Q and H are pump flow and pump pressure difference across the pump, respectively, and a_i and b_i are coefficients. Note that in practical exercise, model (3) can provide estimates of the pump flow and pressure difference across the pump without implanted sensors (pressure and flow sensors) from the measurable variables I and ω [5]. We assume the pump flow and the pressure difference across the pump are available for the purpose of the characterization study of the pump operation.

3. CHARACTERIZATION OF THE PUMP OPERATING STATUS

In this section, the pump operating status will be characterized to provide accurate information to control the pump speed without introducing suction in the left ventricle. With the different pump speeds, the pump flow and pump pressure difference indicate the various information under diverse operating conditions. Since the pump is implanted for the patient whose heart is not healthy, the diverse heart contractilities can indicate a variety of weak heart

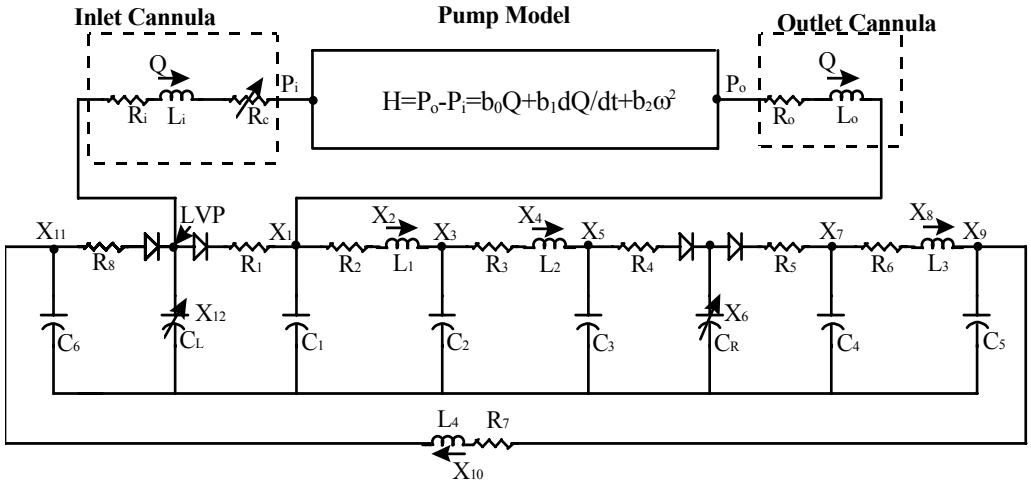

Fig. 1. Model of a cardiovascular system with an implanted LVAD.

conditions of the patient. As the value of the E_{max} for the left ventricle in (2) represents the strength of the contractility of the left ventricle, the different values of E_{max} indicate the diverse contractilities of the patient's heart. Note that for a normal heart, E_{max} of the left ventricle is set 1.9 in Fig. 1 and the smaller value of E_{max} for the left ventricle represents the weak heart condition. Without pump support, while E_{max}=1.9 for a normal heart provides 85.82 mmHg of the mean aorta pressure and 4.88 L/min of the mean cardiac output, E_{max} =0.6 provides 59.5 mmHg of the mean aortic pressure and 3.37 L/min of the mean cardiac output. This indicates that E_{max} =0.6 does not provide proper cardiac output at adequate pressure perfusion.

With the implanted blood pump, the physiological variables change as the pump speed changes. In many patients, the weak contractility of the natural heart during the pump support contributes to the pulsatility of the hemodynamic signals of left ventricle pressure, aorta pressure, pump flow, and pressure difference across the implanted pump. The pulsatility index of the signal is defined to represent the amplitude of the hemodynamic signal as

$$S_{pul}(t) = G_l(abs(G_h(S(t)))),$$

where G_l and G_h are low-pass and high-pass filters with cutoff frequencies of 0.25 Hz and 0.75 Hz, respectively, and S_{pul} is the pulsatility index of the pulsatile signal S [4]. To describe the characterization of the pump operating status, we define a pulsatility ratio as

$$R_{pul} = \frac{Q_{pul}}{\Delta P_{pul}}, \tag{4}$$

where R_{pul} is the pulsatility ratio, Q_{pul} is the pulsatility index of the pump flow Q, and ΔP_{pul} is a pulsatility index of the pressure difference H across the pump, respectively. The pulsatility indices Q_{pul} and ΔP_{pul} are given as

$$Q_{pul}(t) = G_l(abs(G_h(Q(t)))),$$

$$\Delta P_{pul}(t) = G_l(abs(G_h(H(t)))).$$

Note that while units of pulsatility of the pump flow and pressure difference follow units of the pump flow and pressure difference, respectively, units of pulsatility of signals will not be explicitly indicated.

The pulsatility controller in [4] adjusts the pump speed to regulate the pulsatility index of the pump flow according to the reference pulsatility index. That is, the controller adjusts the pump speed to maintain the amplitude of the pump flow according to the reference pulsatility index. The pulsatility index of the pump flow can be expressed in terms of the amplitude of the pulsatile flow Q as [9]

$$Q_{pul} \approx 0.636 Q_{amp}, \tag{5}$$

where Q_{amp} is an approximate amplitude of the pulsatile pump flow Q. For example, if we choose the reference pulsatilities Pul_{ref} = 20 and Pul_{ref} = 15, then the controller adjusts the pump speed to achieve approximately 31.4 and 22.7 of the amplitude of the pump flow Q, respectively. Furthermore, since the contractility of the left ventricle contributes to the pulsatility of the hemodynamic signals, a choice of the reference pulsatility index of the pump flow implicitly indicates a reference of the peak LVP. The relationships between the pulsatility indices of the pump flow and pressure difference and the peak of the LVP can be found in [9]. The pulsatility controller requires a carefully chosen set-point of the reference pulsatility index to properly adjust the pump speed without introducing suction in the left ventricle. The misleading set-point of the pulsatility controller causes suction in the left ventricle. In this section, we utilize disadvantages of the pulsatility controller to examine the properties of the pump operating characteristics in terms of the pulsatility ratio in (4).

The pulsatility controller in [4] and a combined model of a cardiovascular system and an implanted pump in Fig. 1 were both implemented in MATLAB (Mathworks, Natick, MA.) and simulations were performed to illustrate the pump operating characteristics under diverse conditions. The maximum elastance of the left ventricle E_{max} was set to represent the weakness of the heart and the different values of the reference control index of the pulsatility controller were used to investigate the hemodynamic response and to characterize the pump operating status. Also, the change in the systemic vascular resistance (SVR, R_3 in Fig. 1) was included to represent any physical change in the body. In simulations, the pulsatility controller adjusted the pump speed according to the reference pulsatility index of the pump flow. The initial pump speed was set to 838 rad/sec (minimal pump speed) and maintained for 20 sec to ensure the convergence of the pulsatility index algorithm. After 20 sec, the controller began to change the pump speed to reach the steady state. At 80 sec, SVR change was made and the simulation was continued for another 80 sec to provide the steady state response to the new parameter value.

3.1. Weak heart with E_{max} = 0.6 of the left ventricle

The natural heart was impaired to adjust E_{max} of the left ventricle 0.6 from the normal value 1.9. With this impaired contractility of the left ventricle, the two reference pulsatility indices (Pul_{ref} = 20 and 15) of the pump flow were used to investigate the characteristics of the pump operating status.

A) Reference pulsatility index Pul_{ref} = 20

As the controller adjusts the pump speed to support the natural heart, the physiological variables change

according to the reference pulsatility index of the pump flow. Fig. 2 shows the physiological variables such as the pump speed, aortic pressure (AoP), left ventricle pressure (LVP), and left atrium pressure (LAP) as the pulsatility controller adjusts the pump speed according to the reference pulsatility index Pul_{ref} = 20. While the controller adjusts the pump speed, the physiological variables such as AoP, LVP, and LAP maintain the blood and pressure perfusion to the body without introducing suction in the left ventricle. As SVR changes at 80 sec, the cardiovascular system requires a change in the pump operating speed to maintain the blood and pressure perfusion and the controller adjusts the pump speed according to the reference pulsatility index to compensate for changes in the physiological needs. The resulting AoP becomes higher and LAP and LVP maintain the previous values, which resembles the Starling response of the natural heart.

Fig. 3 illustrates trajectories of the pump flow and

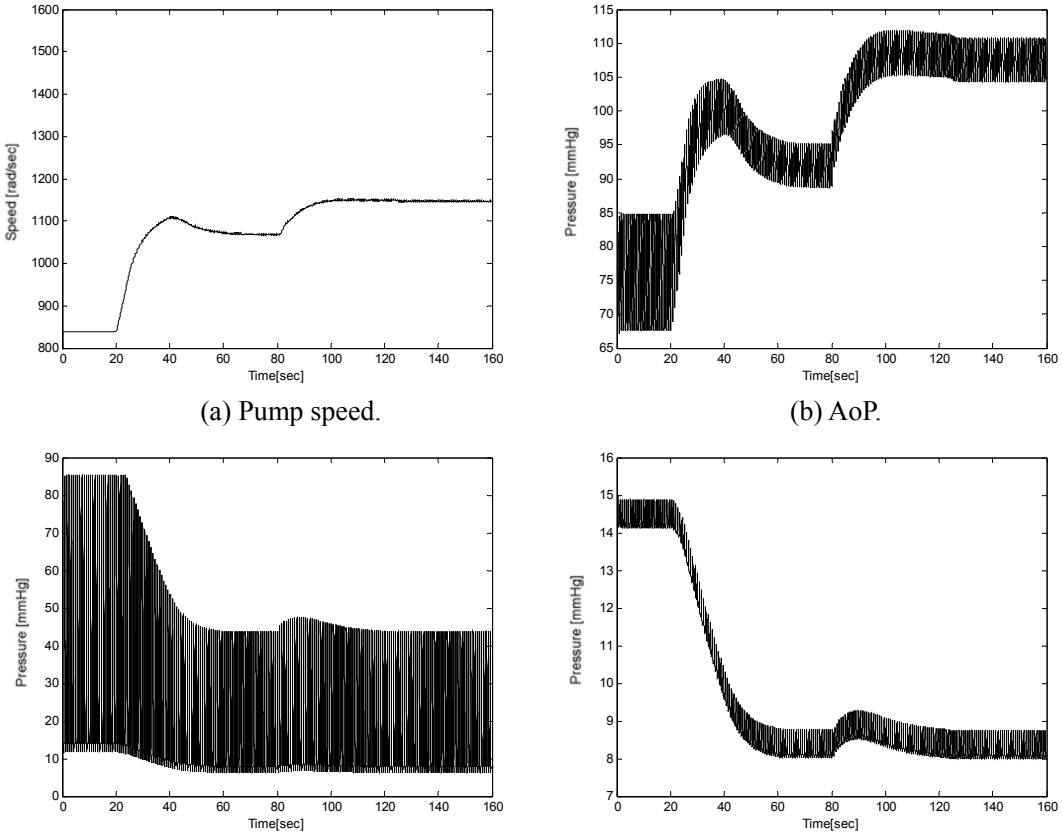

(a) Pump speed. (b) AoP.

(c) LVP. (d) LAP.

Fig. 2. Responses of the physiological variables under reference pulsatility index 20 for a weak heart.

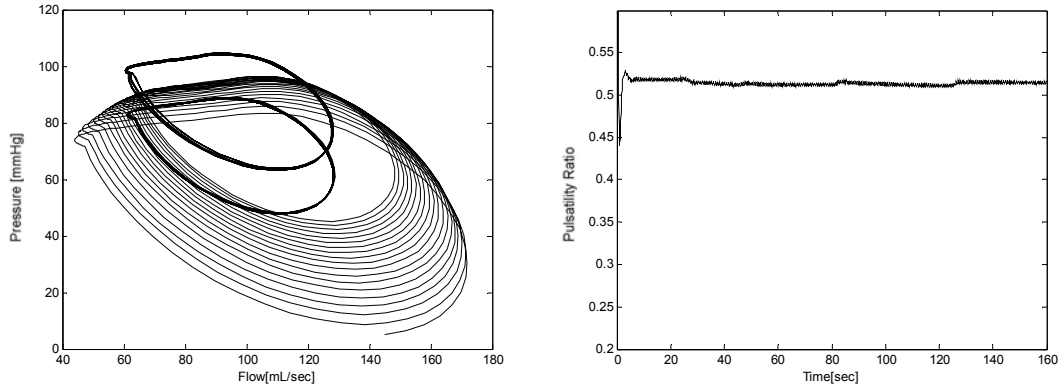

(a) (b)

Fig. 3. Pump operating characteristics under reference pulsatility index 20 for a weak heart. (a) The trajectories of the pump characteristics (b) Pulsatility ratio.

the pressure difference across the pump, and the pulsatility ratio R_{pul}. To plot Fig. 3(a), parts of the trajectories are selected to reduce the complexity and show the distinct characteristics of the pump. In Fig. 3(a), the pump flow maintains pulsatility according to the reference pulsatility index and the pressure difference also maintains its pulsatility. As the pump speed increases, the trajectory loops of the pump flow and pressure difference across the pump maintain the shape of the "distorted water drop" but become smaller in size. As SVR changes, the trajectory loops (bold-line trajectory loops in Fig. 3(a)) slightly move to the other region while preserving the shape of "distorted water drop". In Fig. 3(b), the resulting pulsatility ratio R_{pul} is maintained at about 0.52 even when change in SVR occurs at 80 sec.

B) Reference pulsatility index Pul_{ref} = 15

Fig. 4 shows resulting physiological variables such as the pump speed, AoP, LVP, and LAP. The controller increases the pump speed from the minimal pump speed to regulate the pulsatility index of the pump

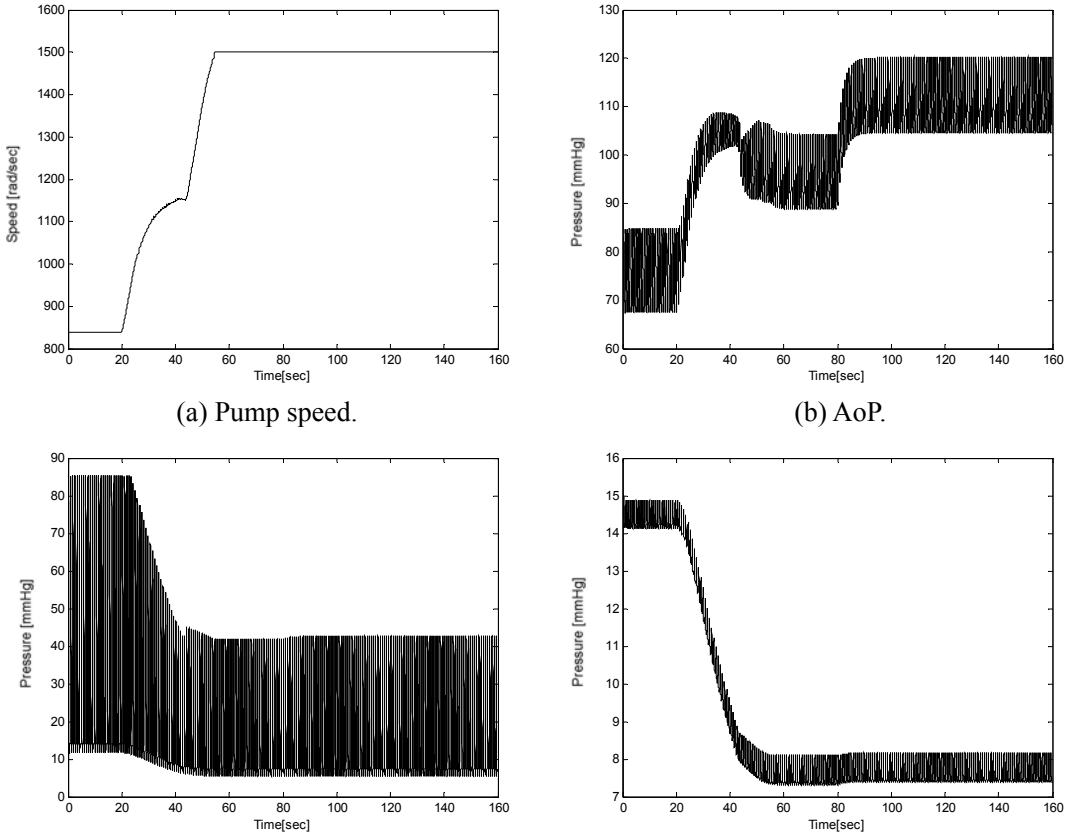

(a) Pump speed. (b) AoP.

(c) LVP. (d) LAP.

Fig. 4. Responses of the physiological variables under reference pulsatility index 15 for a weak heart.

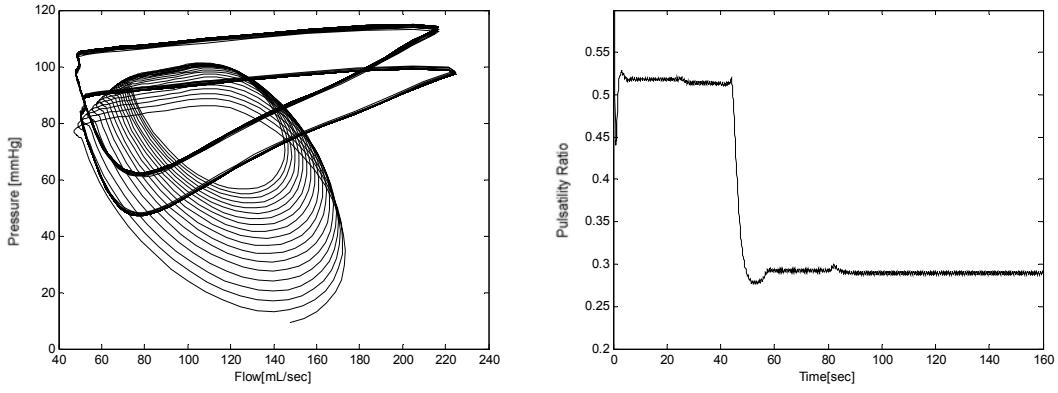

(a) (b)

Fig. 5. Pump operating characteristics under reference pulsatility index 15 for a weak heart. (a) The trajectories of the pump characteristics (b) Pulsatility ratio.

flow according to the reference pulsatility index. As the controller increases the pump speed, the pulsatility index of the pump flow diminishes and AoP and LVP increases and decreases, respectively, while the pulsatilities of AoP and LVP diminish. However, as the pump speed increases and suction occurs around 40 sec, the pulsatility index of the pump flow does not diminish even with an increase of the pump speed and it requires the controller to increase the pump speed to its maximal speed as shown in Fig. 4(a). As suction occurs, the pulsatilities of AoP and LVP do not diminish with an increase of the pump speed as shown in Fig. 4(b)-(c). In Fig. 4(d), LAP also indicates a diminishing pulsatility as the pump speed increases before suction occurrence, but after suction occurrence, LAP maintains definite pulsatility at around 8 mmHg. The pump speed, adjusted by the pulsatility controller with a reference pulsatility index Pul_{ref} = 15, causes suction in the left ventricle and the resulting physiological variables represent the different behaviors from those of the reference pulsatility index Pul_{ref} = 20.

Trajectories of the pump flow and pressure difference across the pump are shown in Fig. 5(a). To plot Fig. 5(a), parts of the trajectories are selected to reduce the complexity and indicate the distinct characteristics of the pump. There are two shapes of trajectory loops for this case. For low pump speed operation, suction does not occur and the pump flow and pressure difference preserve pulsatilities. Since a weak heart can still provide contractility during pump support, the pressure difference across the pump becomes minimal during the systolic period of a cardiac cycle, and becomes maximal during the diastolic period of a cardiac cycle. Similarly, the pump flow reaches its peak during the systolic period of a cardiac cycle, and goes down to its lowest point during the diastolic period of a cardiac cycle. This phenomenon reflects characteristics of the pump operating conditions and presents pulsatilities of the pump flow and pressure difference across the pump. The shape of the trajectory loops prior to suction occurrence is similar to the "distorted water drop" and becomes smaller in size with an increase of the pump speed.

With an increase of the pump speed and suction occurrence, the pump flow and the pressure difference do not preserve their own pulsatilities and the shapes of the trajectory loops of the pump flow and pressure difference change from the "distorted water drop" shape to that of the "distorted triangle". Fig. 5(b) clearly indicates the change in the pump characteristics in terms of the pulsatility ratio R_{pul}. There is an abrupt change in the pulsatility ratio from about 0.52 to 0.29. This change coincides with the physiological status change in the patient's cardiovascular system from "before suction" to "suction". For the normal pump operation, the pulsatility ratio maintains about 0.52. As suction occurs due to an excessive pump speed, the pulsatility ratio begins to sharply decrease to 0.29. The pulsatility ratio maintains about 0.29 during the "suction" status of pump operation.

3.2. Weaker heart with E_{max} = 0.4 of the left ventricle

Previously, we set the contractility of the left ventricle at E_{max} = 0.6 to accommodate the weak heart condition. To provide a more diverse situation, we repeatedly investigated the characteristics of the pump operating condition for a weaker heart at E_{max} = 0.4 of the left ventricle contractility. As the weaker heart generates weaker pulsatility of the physiological variables, the reference pulsatility indices should be set to be smaller values to provide a greater range of pump speed change and resulting cardiac output. Next, we examine the physiological responses of the cardiovascular system under the diverse reference pulsatility indices for different heart weakness.

A) Reference pulsatility index Pul_{ref} = 15

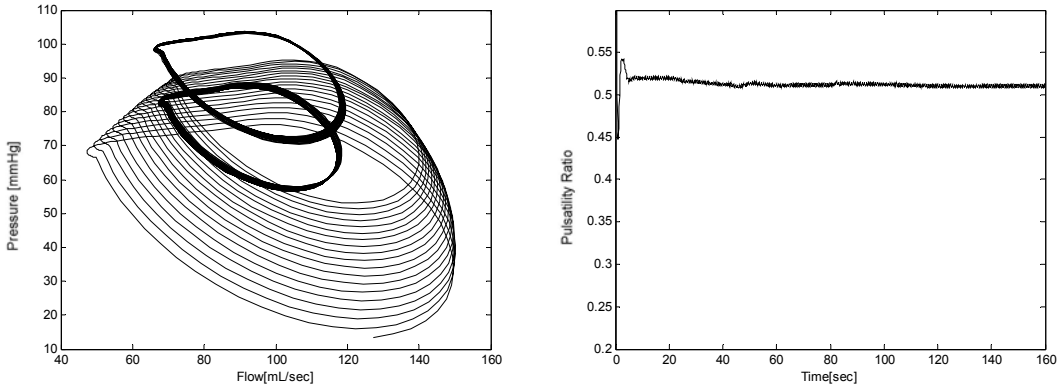

(a) (b)

Fig. 6. Pump operating characteristics under reference pulsatility index 15 for a weaker heart. (a) The trajectories of the pump characteristics (b) Pulsatility ratio.

The controller regulates the pump speed according to the reference pulsatility index. The resulting physiological behaviors such as the pump speed, AoP, LVP, and LAP are not shown in the Figs. but are similar to those of Section 3.1. (See Fig. 2.) The controller does not introduce suction in the left ventricle and it provides the proper blood and pressure perfusion to the body. The corresponding pump flow and pressure difference are presented in Fig. 6(a). To plot Fig. 6(a), parts of the trajectories are selected to reduce the complexity and show the distinct characteristics of the pump. The pump flow and pressure difference preserve their pulsatilities over cardiac cycles and the shape of the trajectory loops of the pump operating characteristics is similar to the "distorted water drop" while it becomes smaller in size with an increase of the pump speed. The two bold-line trajectory loops are due to change in SVR while adjusting the pump speed according to the reference pulsatility index.

Fig. 6(b) indicates that the pulsatility ratio maintains about 0.52 even in the event of SVR change. Note that for the weak heart E_{max} = 0.6, the controller with the reference pulsatility index Pul_{ref} = 15 causes suction in the left ventricle. It is important to recognize that the controller with Pul_{ref} = 15 does not introduce suction for the weaker heart E_{max} = 0.4, but it preserves pulsatilities of the pump flow and pressure across the pump, and maintains the resulting pulsatility ratio of 0.52.

B) Reference pulsatility index Pul_{ref} = 12.5

The physiological behaviors of variables (the pump speed, AoP, LVP, and LAP) under the control condition of the reference pulsatility index Pul_{ref} = 12.5 are not shown in the Figs. but are similar to those discussed in the previous Section 3.1. (See Fig. 4.) Unlike the case of the reference pulsatility index Pul_{ref} =15, the controller does not achieve a satisfying performance with an occurrence of suction in the left ventricle. Fig. 7 indicates corresponding trajectories of the pump flow and pressure difference across the pump, and the pulsatility ratio R_{pul}. As in the suction case in 3.1 (contractility of the left ventricle E_{max} = 0.6 and reference pulsatility index Pul_{ref} = 15), the trajectory loops of the pump flow and pressure difference also reveal two shapes as shown in Fig. 7(a). To plot Fig. 7(a), parts of the trajectories are selected to reduce the complexity and illustrate the distinct characteristics of the pump. Before suction occurs with a low pump speed, trajectory loops of the pump flow and pressure difference appear as the "distorted water drop" and the size of the trajectory loops becomes smaller with an increase of the pump speed. With an increase of the pump speed and suction occurrence, the shape of trajectory loops changes from the "distorted water drop" shape to that of the "distorted triangle". The two bold-line trajectory loops of the "distorted triangle" are due to change in SVR. In Fig. 7(b), the pulsatility ratio indicates a sudden change as suction in the left ventricle occurs. While the pulsatility ratio maintains about 0.52 for the normal pump operation, it abruptly decreases to 0.22, where it maintains during the pump operating status of "suction".

4. DISCUSSIONS

The pump operating characteristics have been investigated in terms of the pulsatility ratio of the pulsatility index of the pump flow to the pulsatility index of the pressure difference across the pump. The pulsatility controller in [4] uses the properties of the diminishing pulsatility of the pump flow before suction occurrence and provides the speed regulation to maintain the pulsatility index of the pump flow according to the reference pulsatility index of the pump flow. The pulsatility controller using the pulsatility index of the pump flow has potential limitations. One value of the pulsatility index of the

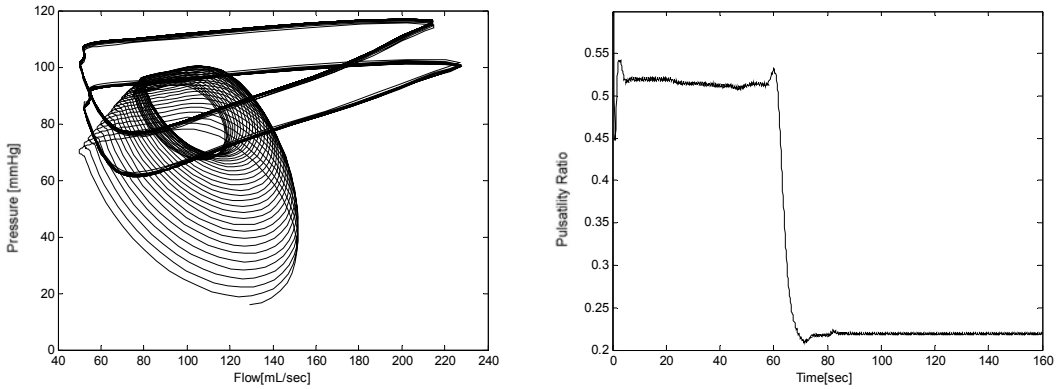

(a) (b)

Fig. 7. Pump operating characteristics under reference pulsatility index 15 for a weaker heart. (a) The trajectories of the pump characteristics (b) Pulsatility ratio.

Table 1. Comparison of pulsatility ratio for diverse reference pulsatility indices and heart conditions.

		Conditions			
		Weak heart E_{max} = 0.6		Weaker heart E_{max} = 0.4	
		Pul_{ref} = 20	Pu_{lref} = 15	Pul_{ref} = 15	Pul_{ref} = 12.5
Pulsatility ratio (approximation)	Suction occurrence	X	O	X	O
	No suction	5.2	5.2	5.2	5.2
	Suction		0.29		0.22

pump flow can indicate both "before suction" and "suction" of the pump operation. Also, the reference pulsatility index for the controller is not clearly assigned since it depends on the conditions of the patients. The reference pulsatility index should be carefully chosen to provide proper blood at adequate perfusion pressure to the body while avoiding suction in the left ventricle. It is necessary to investigate a control index of a pump controller to alleviate the limitations of the pulsatility controller.

As a control index to compensate for the limitations of the pulsatility controller, the pulsatility ratio reveals a unique characteristic to classify the pump operating status such as "before suction" and "suction". In Section 3, the pulsatility controller using the pulsatility index of the pump flow shows diverse physiological responses to different reference pulsatility indices for the diverse patients' conditions in terms of the pulsatility ratio. The results are summarized in Table 1. In Table 1, the pulsatility ratios are about 0.52 before suction occurs in the left ventricle regardless of the patients' contractilities. The pulsatility ratios change to about 0.29 or 0.22 from about 0.52 as suction occurs. As the pulsatility ratio demonstrates distinction between the normal pump operation and suction status of the pump, it can identify suction occurrence in the left ventricle regardless of the patients' weak heart contractilities with a single value. The pulsatility ratio can alleviate the limitations of the pulsatility controller and can be used as a control index for the controller to regulate the pump speed without introducing suction in the left ventricle under the diverse heart conditions of various patients. Also, the pulsatility ratio can provide an opportunity for the controller to challenge the very weak heart conditions of the patients that the pulsatility controller cannot handle due to the resulting weak pulsatility of the pump flow. The development of the controller using the pulsatility ratio of the pump characteristics as a control index is an ongoing study.

REFERENCES

[1] D. B. Olsen, "The history of continuous-flow blood pumps," *Artificial Organs*, vol. 24, no. 6, pp. 401-404, 2000.

[2] H. Schima, W. Trubel, A. Moritz, G. Wieselthaler, H. G. Stöhr, H. Thomas, U. Losert, and E. Wolner, "Noninvasive monitoring of rotary blood pumps: Necessity, possibilities, and limitations," *Artificial Organs*, vol. 6, pp. 195-202, 1992.

[3] J. R. Boston, M. A. Simaan, J. F. Antaki, Y. Yu, and S. Choi, "Intelligent control design for heart assist devices," *Proc. of 1998 ISIC/CIRA/ISAS Joint Conference*, pp. 497-502, Gaithersburgh, MD, 1998.

[4] S. Choi, J. F. Antaki, J. R. Boston, and D. Thomas, "A sensorless approach to control of a turbodynamic left ventricular assist system," *IEEE Trans. on Control Systems Technology*, vol. 9, no. 3, pp. 473-482, 2001.

[5] S. Choi, J. R. Boston, D. Thomas, and J. F. Antaki, "Modeling and identification of an axial flow blood pump," *Proc. of America Control Conference*, vol. 6, pp. 3714-3715, Albuquerque, NM, 1997.

[6] S. Choi, "Suction detection in left ventricular assist system: data fusion approach," *International Journal of Control, Automation, and Systems*, vol. 1, no. 3, pp. 368-375, September 2003.

[7] J. R. Boston, L. Baloa, Dehou Liu, M. A. Simaan, S. Choi, and J. F. Antaki, "Combination of data approaches to heuristic control and fault detection," *Proc. of IEEE Conference on Control Applications and International Symposium on Computer-Aided Control Systems Design*, pp. 98-103, Anchorage, AK, September 25-27, 2000.

[8] M. Vollkron, H. Schima, L. Huber, R. Benkowski, G. Morello, and G. Wieselthaler, "Development of a suction detection system for axial blood pumps," *Artificial Organs*, vol. 28, no. 8, pp. 709-716, 2004.

[9] S. Choi, *Modeling and Control of Left Ventricular Assist System*, Ph.D. Dissertation, University of Pittsburgh, 1998.

[10] G. Avanzolini, P. Barbini, A. Cappello, and G. Cevenini, "CADCS simulation of the closed-loop cardiovascular system," *Int. J. Biomed*

Comput, vol. 22, pp. 39-49, 1988.

[11] H. Schima, J. Honigschnabel, W. Trubel, and H. Thoma, "Computer simulation of the circulatory system during support with a rotary blood pump." *Trans. Am. Soc. Artif. Org.*, vol. 36, pp. M252-M254, 1990.

Seongjin Choi received the B.S. and M.S. degrees in Electrical Engineering from Korea University, Korea, in 1984 and 1986, respectively, and the Ph.D. degree in Electrical Engineering from the University of Pittsburgh, Pittsburgh, PA, in 1998. He is currently an Assistant Professor in the Department of Electronics and Information Engineering at Korea University, Korea. His research interests are in the area of modeling and control of biomedical systems.

J. Robert Boston received the B.S. and M.S. degrees in Electrical Engineering from Stanford University, Stanford, CA, in 1964 and 1966, respectively, and the Ph.D. degree from Northwestern University, Evanston, IL, in 1971. Dr. Boston has held faculty appointments at the University of Maryland, Carnegie Mellon University, and the University of Pittsburgh School of Medicine. He is currently a Professor and Undergraduate Coordinator in the Department of Electrical Engineering at the University of Pittsburgh. His interests are in the areas of biomedical signal processing, processing of speech signals by the auditory system, and fuzzy signal detection. His current research projects include the development of image analysis techniques for the study of biomechanics of motion in patients with lower back pain (in collaboration with Thomas Rudy, Ph.D., of the Pain Evaluation and Treatment Institute, University of Pittsburgh), identification of speech components using wavelets, modeling active hair cell processes in the cochlea, and development of control systems for artificial organs.

James F. Antaki is an Associate Professor of Biomedical Engineering with a courtesy appointment in Computer Science at Carnegie Mellon University. He also holds academic positions in the Departments of Surgery and Bioengineering at the University of Pittsburgh. He received a BS in Mechanical and Electrical Engineering from Rensselaer Polytechnic Institute (1985) and a Ph.D. in Mechanical Engineering from the University of Pittsburgh (1991). Over the past 12 years, he has conducted research in the field of prosthetic cardiovascular organs. In 1997, his team completed the development of a novel magnetically levitated turbodynamic blood pump, the *Streamliner*, which recorded the world's first in-vivo implant of such a device, and was granted an IEEE Controls Systems Technology Award in 2001. Since migrating to Carnegie Mellon, he has intensified his interest in advancing the methodology by which medical devices are designed. He has recently founded the Laboratory for Innovation and Optimization of Medical Devices which seeks to promote creative collaborations between medical professionals, industrial partners, and faculty experts in the field of design.

Dr. Antaki holds twelve patents related to artificial organs and four in other fields. He was recently recognized by as one of the top 40 most influential people under age 40 in the Pittsburgh region. For the past three years, Dr. Antaki has been teaching the capstone design course within the Department of Bioengineering. He is a proponent of teaching methods that promote the integration of didactic coursework with industrial mentorship, aimed at solving practical problems in biomedicine, with particular emphasis on engineering of medical devices.